Protonation Dynamics and Hydrogen Bonding in Aqueous Sulfuric Acid

ARTICLE *in* THE JOURNAL OF PHYSICAL CHEMISTRY B · AUGUST 2015

Impact Factor: 3.3 · DOI: 10.1021/acs.jpcb.5b04371 · Source: PubMed

THE JOURNAL OF PHYSICAL CHEMISTRY B

Article

pubs.acs.org/JPCB

Protonation Dynamics and Hydrogen Bonding in Aqueous Sulfuric Acid

Johannes Niskanen,[*,†] Christoph J. Sahle,[†,‡] Iina Juurinen,[†] Jaakko Koskelo,[†] Susi Lehtola,[†,§] Roberto Verbeni,[‡] Harald Müller,[‡] Mikko Hakala,[†] and Simo Huotari[†]

[†]Department of Physics, University of Helsinki, P.O. Box 64, FI-00014 Helsinki, Finland

[‡]ESRF—The European Synchrotron, CS40220, 38043, Grenoble Cedex 9, France

Supporting Information

ABSTRACT: Hydration of sulfuric acid plays a key role in new-particle formation in the atmosphere. It has been recently proposed that proton dynamics is crucial in the stabilization of these clusters. One key question is how water molecules mediate proton transfer from sulfuric acid, and hence how the deprotonation state of the acid molecule behaves as a function concentration. We address the proton transfer in aqueous sulfuric acid with O K edge and S L edge core-excitation spectra recorded using inelastic X-ray scattering and with *ab initio* molecular dynamics simulations in the concentration range of 0−18.0 M. Throughout this range, we quantify the acid−water interaction with atomic resolution. Our simulations show that the number of donated hydrogen bonds per O_{water} increases from 1.9 to 2.5 when concentration increases from 0 to 18.0 M, in agreement with a rapid disappearance of the pre-edge feature in the O K edge spectrum. The simulations also suggest that for 1.5 M sulfuric acid SO_4^{2-} is most abundant and that its concentration falls monotonously with increasing concentration. Moreover, the fraction of HSO_4^- peaks at ∼12 M.

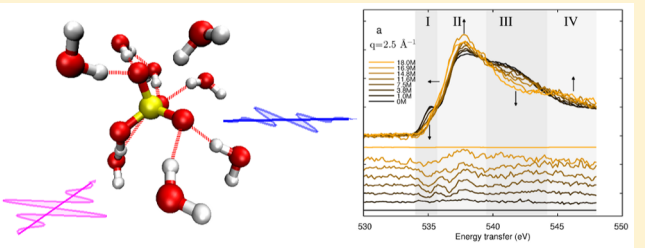

INTRODUCTION

Sulfuric acid is generated in the atmosphere by oxidation of SO_2 which originates both from human activity and natural sources. Being highly hygroscopic, sulfuric acid has been identified as one of the main driving compounds in atmospheric nucleation, i.e., formation of new particles,[1,2] which cause a net climate cooling effect.[3] To yield significant nucleation rates, sulfuric acid requires other chemical substances to stabilize the forming clusters, and intense theoretical work has been devoted to studies of the few-molecule sulfuric acid based systems (for example, refs 4−25 and references therein). Typical theoretical approaches rely on quantum chemistry and minimum-energy structures. However, recently the dynamical aspects of nucleation of small clusters were addressed using first-principles calculations[26,27] that revealed a competition over the control of proton, an aspect requiring experimental confirmation. In addition to a large number of theoretical studies of small acid−water clusters, microwave, infrared (IR), optical, vacuum ultraviolet (VUV), and soft X-ray spectroscopy has been applied to study the structure and protonation state of the acid molecules in gas and in liquid phase.[28−35]

Simulations on liquid sulfuric acid[36−41] address the protonation process and the molecular-ion structures present in the solution. Stepwise dissociation was evaluated critically by Fraenkel,[42,43] who proposed formation of H_4SO_5 for concentrations up to 6.9 M.

In this article, we study the problem of protonation state distribution by ab initio molecular dynamics simulations and compare the results to those obtained experimentally by using a novel tool, namely nonresonant inelastic X-ray scattering (NRIXS).[44] The NRIXS spectra from core−electron excitations provide fingerprints of the element-specific local chemical environment, which allows accurate studies of chemical processes. Combining simulations and experiments, we deduce the quantitative details of the hydrogen bonding in water and protonation states of acid molecules throughout the whole concentration range from pure water to highly concentrated acid. To our knowledge, ab initio molecular dynamics simulations of this extensivity have not been published before. Utilization of NRIXS core-level excitations allows us to study local atomistic structure of the molecular liquid in an previously unseen fashion, relating the spectral information to atomistic structure near the excited site.

METHODS

Spectroscopy. In NRIXS, high-energy (∼10 keV) X-rays (energy ω_1) scatter inelastically from the sample, and the energy-loss spectra of the scattered photons (ω_2) are recorded. The spectra depend on the transferred energy $\omega = \omega_1 - \omega_2$ and momentum $\mathbf{q} = \mathbf{k}_1 - \mathbf{k}_2$, where $\mathbf{k}_{1,2}$ are the wave vectors of the

Received: May 7, 2015
Revised: August 17, 2015

DOI: 10.1021/acs.jpcb.5b04371
J. Phys. Chem. B XXXX, XXX, XXX−XXX

incident and scattered photons, respectively. The spectra are described by the so-called double differential cross section[44]

$$\frac{d^2\sigma(\mathbf{q}, \omega)}{d\Omega\, d\omega_2} = \left(\frac{d\sigma}{d\Omega}\right)_{Th} \langle S(\mathbf{q}, \omega, \mathbf{R})\rangle_{NPT} \quad (1)$$

where $(d\sigma/d\Omega)_{Th}$ is the Thomson scattering cross section and $S(\mathbf{q},\omega,\mathbf{R})$ is the dynamic structure factor of the studied system with nuclear coordinates $\mathbf{R}$. Since each ensemble configuration $\mathbf{R}$ with one excited atomic site yields an individual spectrum, the local chemical structure around a chosen element can, in principle, be interpreted in terms of the spectral features. The Thomson scattering cross section depends only on ω_1 and ω_2, and on the polarizations of the photons $\mathbf{e}_1$ and $\mathbf{e}_2$, whereas the dynamic structure factor gives the information on the system under study.

As both incoming and outgoing photons are hard X-rays, the momentum $\mathbf{q}$ transferred to the sample can be significant. Therefore, one can tune the technique for sensitivity between dipole and higher-order multipole transitions. For small values of q, dipole transitions dominate. For large q, the spectrum manifests also high-order multipolar (dipole-forbidden) transitions.

Owing to the low absorption cross section in the 10 keV range, the NRIXS technique allows using sample environments impermeable for soft X-rays, and measurements in ambient (and even extreme) conditions are possible. Unlike the soft X-ray techniques that require vacuum environments, the NRIXS experiments are therefore performed in well-defined thermodynamic conditions. Our experiments were done at room temperature and pressure, making the experiment probe the ensemble average $\langle\ \rangle_{NPT}$ of eq 1. Owing to these features NRIXS provides a unique technique the advantages of which were lately manifested, for example, in our recent works with high-temperature CO_2[45] and supercritical water.[46]

Experiment. The experiment was performed for solutions of H_2SO_4 concentrations of 0 M (pure water), 1, 3.8, 7.5, 11.6, 14.8, 16.9, and 18.0 M at the inelastic X-ray scattering beamline ID20 of the European Synchrotron Radiation Facility.[47] The measurements were carried out by recording the S intensity of scattered photons with a fixed energy 9.7 keV while scanning the incident photon energy between 9.7−10.3 keV covering energy transfers between 0−0.6 keV required for the S $L_{2,3}$ edge and the O K edge excitations. The repetitively recorded raw spectra were normalized by the beam-intensity monitor, after which they were checked for internal consistency, and finally averaged to yield the final spectra. The energy resolution of the experiment was 0.6 eV. The spectra were recorded for momentum transfers of $q \approx 2.5$ Å^{-1} (referred to as "low-q"), and $q \approx 9$ Å^{-1} ("high-q").

Sulfuric acid with 18.0 M was provided by Carlo Erba Reagents, and solutions with lower concentrations were provided by Carl Roth. The commercially provided solutions were used without further processing, except for the 14.8 M (79 m-%) solution, which was prepared using the 11.6 M (62 m-%) and the 18.0 M (96 m-%) solutions. Pure H_2O was measured using Milli-Q water (Millipore Corporation). The samples were injected to glass mark tubes and formation of beam-damage was circumvented by oscillatory movements of the sample in the vertical direction in order to decrease the dose rate per volume element.

Structural Simulations. We performed *ab initio* molecular dynamics (AIMD) simulations for 7 different concentrations modeled by combinations (0, 64), (1, 63), (6, 54), (12, 36), (20, 20), (21, 7) and (24, 0) of acid and water molecules (#acid, #water) in the simulation box. The choice corresponds to the molarities 0, 1.5, 7.1, 12.1, 15.8, 17.7, and 18.8 M. The *NVT* ensemble was sampled utilizing massive Nose−Hoover thermostatting to drive the system to, and keep it in equilibrium at T = 300 K with periodic boundary conditions. After thermalization, 10 ps trajectories were sampled in the production run. The simulations had conserved-energy drifts below 2.6×10^{-6} au/atom/ps indicating good numerical stability.[48] The CP2K code package[49,50] and the Perdew−Burke−Ernzerhof (PBE) exchange-correlation functional[51] were used in the calculations. For the AIMD, polarized valence triple-ξ (TZVP) basis sets[52] and Goedecker−Teter−Hutter (GTH) pseudopotentials[53] were used. Except for the pure H_2O, the simulations were performed in both restricted-Kohn−Sham (RKS) and unrestricted-Kohn−Sham (UKS) frameworks to map the effects of static correlation in the bond forming and breaking processes. The time step used in the AIMD simulation was 0.5 fs.

Classical MD using force field by Loukonen et al.[20] was performed prior to AIMD. The classical MD serves as removing hot spots and as a "rough equilibration" in the simulation before the costly AIMD. After a nanosecond-range classical MD, the AIMD was run then 20 ps before the production runs. In classical MD a protonation state needed to be chosen for the acid molecules, and HSO_4^- + H_3O^+ was assumed as long as there were enough water molecules to accept a proton. For the higher concentrations H_2SO_4 was assumed for the rest of acid molecules.

For the deprotonation-state analysis, a proton was considered to be attached to the sulfate if its distance to any of the oxygens in SO_4^{2-} was less than 1.3 Å. This criterion was used also by Choe and co-workers.[36] An oxygen atom was determined to belong to the SO_4^{2-} if its distance to the sulfur atom was at most 2.0 Å. The number of protons in the sulfate ion was evaluated over the trajectories of production runs for each of the simulated concentration.

RESULTS AND DISCUSSION

Structural Simulations. Being an acid, H_2SO_4 deprotonates in water to form HSO_4^- and SO_4^{2-}. On the basis of our simulations we evaluated the percentage of different protonation states presented with standard deviations, given in Table 1. The AIMD runs performed show, expectedly, different protonation states for sulfuric acid in different concentrations. The number of different sulfate-ion-protonation states remained rather constant in the simulation except in the 1.5 M case where there was only one acid molecule in the simulation box, being either HSO_4^- or SO_4^{2-}. The snapshots of the simulation box at the beginning of the RKS production runs are shown in Figure 1.

Choe and co-workers reported AIMD study of H_2SO_4(aq)[36] of two concentrations: 1.5 M (1A, 63W) and 12.1 M (12A, 36W). When comparing the values obtained in this work to theirs, we first observe a drastic difference in the 1.5 M simulation. Instead of singly deprotonated acid, SO_4^{2-} is dominating species in both RKS and UKS runs of this work. In RKS simulations, the protons are found in the first solvation shell, whereas in UKS they are more mobile. Moreover, somewhat differing numbers are obtained also for the 12.1 M system.

DOI: 10.1021/acs.jpcb.5b04371
J. Phys. Chem. B XXXX, XXX, XXX−XXX

Table 1. Fractions of the Protonation States of Sulfate Ions Calculated as Averages from the AIMD Production Runs[a]

concn M (mol %)	H_2SO_4 (mol %)	HSO_4^- (mol %)	SO_4^{2-} (mol %)
		RKS	
1.5 (2)	0 (0) [0.0[b]]	1 (8) [100[b]]	99 (8) [0.0[b]]
7.1 (10)	0 (1)	53 (7)	47 (7)
12.1 (25)	2 (4) [0.0[b]]	82 (7) [89.0[b]]	16 (5) [11.0[b]]
15.8 (50)	23 (6)	74 (7)	3 (3)
17.7 (75)	73 (4)	27 (4)	0 (0)
18.8 (100)	100 (0)	0 (0)	0 (0)
		UKS	
1.5 (2)	0 (0) [0.0[b]]	1 (11) [100[b]]	99 (11) [0.0[b]]
7.1 (10)	0 (2)	35 (13)	65 (13)
12.1 (25)	3 (5) [0.0[b]]	76 (10) [89.0[b]]	21 (9) [11.0[b]]
15.8 (50)	27 (7)	66 (7)	7 (3)
17.7 (75)	74 (4)	26 (5)	0 (1)
18.8 (100)	100 (0)	0 (0)	0 (0)

[a]The standard deviation of the molar percentages is given in parentheses. [b]Choe et al.[36]

Fraenkel has proposed proposed formation of H_4SO_5 for concentrations up to 6.9 M in.[42,43] We evaluated this proposal in our simulations by computing the number of oxygens to each sulfur atom in each of the systems. The distance criteria 2.0 Å for the S−O bond give only 4 oxygen atoms without a single exception in the simulation. However, Fraenkel studied the concentration range from 0 to 6.9 M and therefore the only systems in our simulations that could possibly correspond this range are the 1.5 M (1A, 64W) and 7.1 M (6A, 54W) ones.

The HSO_4^-/H_2SO_4 and HSO_4^-/SO_4^{2-} ratios have been experimentally determined in numerous works.[35,54,55] The core−electron binding energies of $H_2SO_4(aq)$ have been found to exhibit changes for different concentrations,[35] reflecting the protonation state distribution in the system. The article reported slightly different values for the HSO_4^-/SO_4^{2-} ratio than from numerous other experimental studies.

The data are collected in Figure 2 and are presented together with our simulation results mimicking the plot of Margarella and co-workers.[35] The overall agreement of literature values with our simulations is good. However, for low concentrations

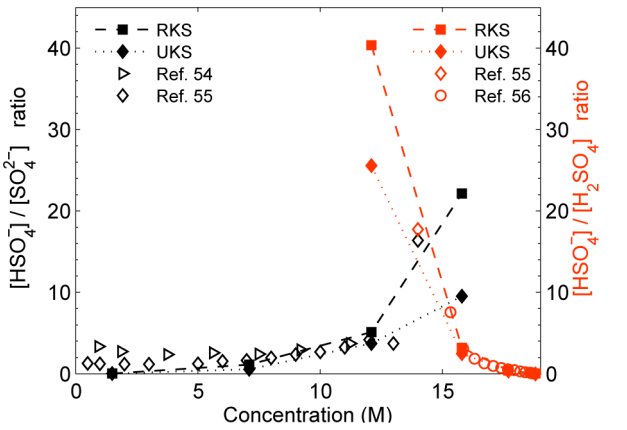

Figure 2. Comparison of protonation-state ratios from our AIMD simulations and references.

the simulations underestimate the $[HSO_4^-]/[SO_4^{2-}]$ ratio, agreeing somewhat better with values obtained by Knopf et al.[54] For 12.1 and 15.8 M the RKS simulation favors singly protonated species yielding higher ratios than UKS.

The number of hydrogen bonds per O_{water} was evaluated from the AIMD trajectories and is depicted in Figure 3. The

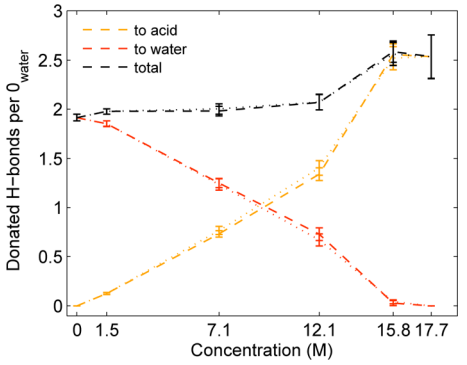

Figure 3. Number of donated H-bonds per O_{water} as a function of concentration according to AIMD simulations. Dashed line shows the results of RKS simulations and dotted line the results of the UKS calculation.

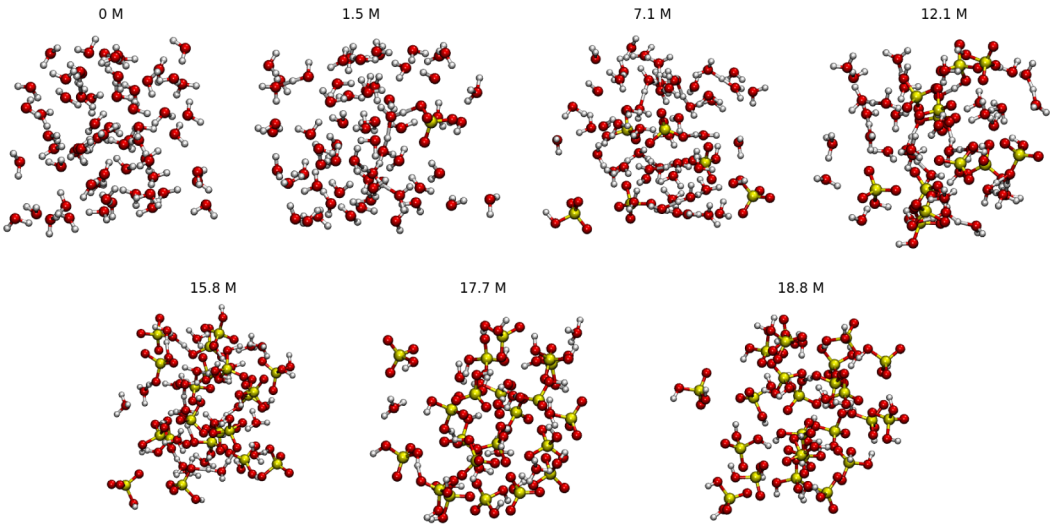

Figure 1. Snapshots of the RKS simulation boxes at the beginning of the production runs. Periodic boundary conditions were applied.

DOI: 10.1021/acs.jpcb.5b04371
J. Phys. Chem. B XXXX, XXX, XXX−XXX

errorbars in the figure show the mean value and the standard deviation. The value changes from ∼1.9 obtained for pure water to ∼2.6 for 17.7 M H_2SO_4(aq) with a step between 12.1 and 15.8 M. The two electron structure methods RKS and UKS give very similar results for hydrogen bonding.

Oxygen K Edge. The recorded O K edge excitation spectra of H_2SO_4(aq) of various concentrations are depicted in Figure 4. The spectra can be divided in four regimes: pre-edge (I), main edge (II), postedge (III), and high-postedge (IV), as indicated by shading in Figure 4. The overall shape of the low-q and high-q spectra are similar. The most pronounced difference is in the pre-edge region, which is enhanced in the high-q spectra. This is because the transitions to s-type final states increase in probability with an increasing q. This spectral feature is due to the water component in the system, and it is absent in pure H_2SO_4. Thus, the pre-edge region allows an indepedent study of the local structure around the water molecules alone.

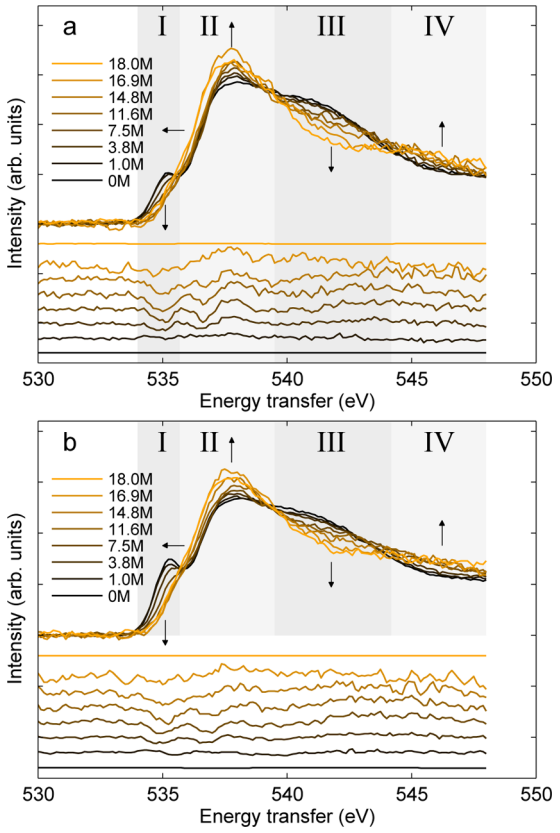

Figure 4. O K edge excitation spectra of H_2SO_4(aq) for different concentrations: the experiment in the dipole-regime (a) and the experiment with q = 9 Å^{-1} (b). The changes in spectral features as a function of increasing concentration are shown with arrows. The residuals of the two-component fit for O K edge excitation spectra of H_2SO_4(aq) for different concentrations, are shown for in the lower parts of the plots. The same scale is used both for the spectra and two-component-fit residuals.

For water and aqueous systems, the correlations between the oxygen K edge spectral features and changes in the molecular structures have been studied extensively.[46,56−66] Although the correlations are not straightforward, it has been shown that the pre-edge is sensitive to the number of hydrogen bonds.[46,58−60,62,63,65] Especially the differences in the donating hydrogen bonds affect the pre-edge.[63] The intensity in the postedge area is related to tetrahedral ordering of the system. This is most prominently seen in hexagonal ice.[56,58,61,64]

The pre-edge feature is seen to weaken with increasing concentration of H_2SO_4, and last signs of it disappear at 7.5 M for low-q and at 11.6 M for high-q spectra. This indicates the propensity of sulfuric acid to establish hydrogen bonds to water molecules, sulfate ion accepting them and water donating them. Although at 7.5 M only 33% of the signal comes from O atoms belonging to the acid molecules, the increase in the hydrogen bond donation by O_{water} molecules readily explains the disappearance of the clear pre-edge shoulder. Our calculations in Figure 3 explain this behavior as an increase of the number of donated hydrogen bonds per O_{water} in region between 7.1 and 15.1 M.

The pre-edge is a feature characteristic to water and related to donating hydrogen bonding in water. As seen in the experiment, the OH group in H_2SO_4 does not exhibit a pre-edge, and therefore H-bonds by this group play no role in formation of pre-edge in the spectrum of pure sulfuric acid. From the data it is impossible to tell whether other structures than water produce a prepeak in intermediate concentrations, but we note that for the rapid disappearance of the prepeak from water this is irrelevant. Namely, the prepeak disappers faster than the ratio of oxygens in water (or H_3O^+) does. If some other structure showed a prepeak, it would mean that the prepeak from water is suppressed even more from pure water case, leading to even stronger conclusion.

The fact that the spectra do not have well-defined isosbestic points indicates that at intermediate concentrations, the solution cannot be a simple binary one. This is naturally to be expected since, in general, all components enlisted in Table 1 should be present in addition to H_2O and H_3O^+. We quantify this by attempting a fit of each experimental spectrum by a superposition of those of pure water and 18.0 M sulfuric acid. The differences between the fit result and spectra are presented in Figure 4. The fit is of course perfect for 0 and 18.0 M, but deviations do appear for all other concentrations. The trend of the failure of such a fit is shown in Figure 5. It depicts the integrated absolute deviation (IAD) of the fit residual as a function of concentration and compares it to the percentage oxygen atoms in HSO_4^- and SO_4^{2-} out of all oxygen atoms in the system, as obtained from the structural simulations. The

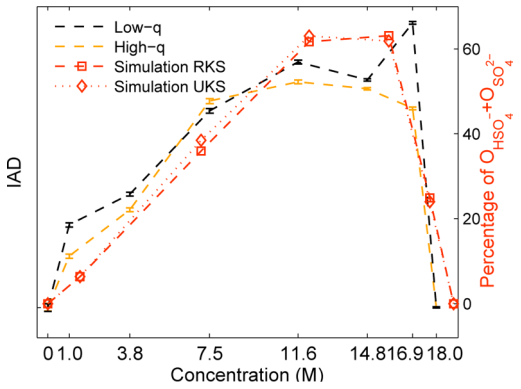

Figure 5. Integrated absolute deviations from the two-component fit. In addition, the percentage of the $O_{HSO_4^-}$ and $O_{SO_4^{2-}}$ in all oxygen atoms in the system according to the simulation is plotted on the right-hand side axis. Statistical errors fit in the marker size for the experiment.

DOI: 10.1021/acs.jpcb.5b04371
J. Phys. Chem. B XXXX, XXX, XXX−XXX

trend of the IAD is seen to follow closely that of the deprotonated-acid-oxygen percentages from the simulation, which shows that the intermediate protonation states is manifested in the spectral residuals. The excellent agreement is a strong evidence that the protonation state of the simulation is reliable within the error bars.

Spectrum calculations for the O K edge were tried using transition potential approximation[67] implemented in the Gaussian and augmented plane wave implementation[68] of CP2K, but the results were found out unsatisfactory. A shift of 4.5 eV between different oxygen sites (i.e., in water or in acid) was obtained, whereas such shift is not seen in the experiment. A shift of this kind could originate, for example, from improper screening of the core site, differently accounted depending on the chemical surrounding of the oxygen atom. However, the problem remains unsolved. The interested reader is recommended to see the Supporting Information for more information.

Sulfur $L_{2,3}$ Edge. The S $L_{2,3}$ edge core-excitation spectra of H_2SO_4(aq) of various concentrations are depicted in Figure 6.

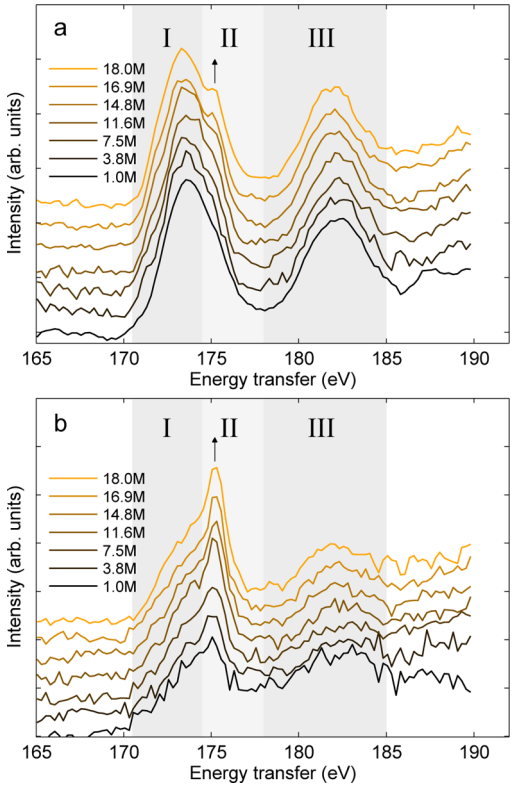

Figure 6. S $L_{2,3}$ edge excitation spectra of H_2SO_4(aq) of different concentrations: the experiment in the dipole-regime (a) and the experiment with q = 9 Å^{-1} (b).

The spectrum can be divided into three regions, two of which contribute bound resonances (I and II), and a shape resonance between 180 and 185 eV (III). The low-q spectrum of Figure 6a does not manifest significant changes as a function of concentration. There is, however, a small shoulder arising in region II at 14.8 M and higher concentrations. The same feature is strongly enhanced in the high-q spectra of Figure 6b, in which case the peak is notably dependent on concentration.

In order to quantify the behavior of this peak, we extracted it by fitting the spectra with five Gaussian and one step function. The peak heights depicted in Figure 7 confirm the raising trend

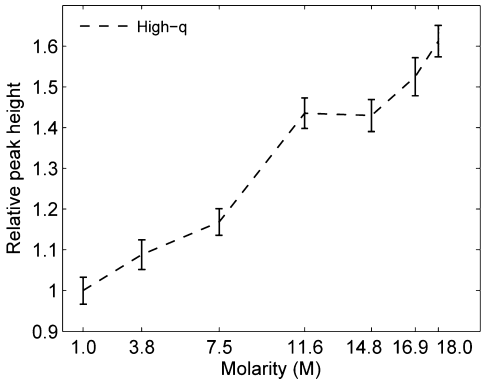

Figure 7. Peak height of S $L_{2,3}$ edge excitation spectra of H_2SO_4(aq) as a function of concentration. The error bars represent the effect of statistical noise in the spectra.

with increasing concentration, and also suggest a jump between 7.5 and 11.6 M. This change takes place in the number of donated hydrogen bonds per water (Figure 3), and is also accompanied by the peak of the presence of singly deprotonated acid (Table 1). This transition point also corresponds the complete hydrogen bonding of water molecules, observed in the O K edge excitations. Overall, the trend in Figure 7 is nearly monotonous, as is the share of fully protonated H_2SO_4 molecules in the liquid. Yet, the H_2SO_4 percentage as a function of concentration is far less linear than the intensity of the peak in region I. Thus, is seems that unlike in the O K edge case, quantitative correspondence to local microscopic structures is not straightforward to obtain from the S $L_{2,3}$ spectra. Below, we present some considerations for their interpretation.

As discussed earlier, one significant property of the NRIXS is its access to dipole forbidden transitions. For the high-q scattering geometry, the higher-order multipoles in the dynamic structure factor of eq 1 dominate, allowing the experiment to probe density of states not accessible with dipole operators—in this case p-type and f-type states. In case of single excited orbital, the spectrum manifests the density of unoccupied states or projected density of unoccupied states (PDOS). In the case of S $L_{2,3}$ edge, the spin−orbit interaction complicates the view somewhat, and we modeled this effect by calculating projected density of transitions (PDOT) which simulates the fact that the unoccupied PDOS is now populated from two spin−orbit split levels. In the calculation of PDOT, the projected density of unoccupied states were shifted by the S 2p spin−orbit splitting, weighting the components 1:2 corresponding the multiplicity of $2p_{1/2}$ and $2p_{3/2}$ states. The projected densities of transitions (PDOT) in 1.5 and 18.8 M solutions were calculated using the Z + 1 approximation to mimic the S 2p core hole, and are depicted in Figure 8, parts a and b. The curves were shifted in energy to match the onset of the S $L_{2,3}$ edge spectrum. Normalization was based on the maxima of the d-type PDOT, mostly responsible for the dipole excitations. This allows interpretation of the high-q spectra with respect to the corresponding low-q ones. The PDOT was obtained as average over 100 structures for both concentrations. The delta-peak PDOT was convoluted with a Gaussian of fwhm 1.5 eV.

As the dipole allowed transitions only probe states with s-type and d-type contributions, the low-q spectra are mostly explained by s + d density of states. The onset of region I contains transitions of s-type but the spectrum is mostly

DOI: 10.1021/acs.jpcb.5b04371
J. Phys. Chem. B XXXX, XXX, XXX−XXX

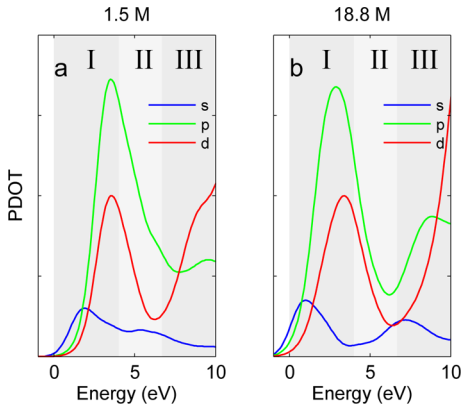

Figure 8. Projected density of transitions (PDOT) for 1.5 M (a) and 18.8 M (b) aqueous sulfuric acid calculated using the $Z + 1$ approximation. The PDOTs were normalized to the maximum for *d*-type, which account for most of the dipole transitions.

dominated by d-type final states. With an increasing q, the higher-order multipole transition operators start to promote transitions to p-type and f-type sates. In this range of q, transitions to f-states are, however, negligible compared to those of the p-states due to a strong spatial overlap of the p final states with the initial 2p wave function.

Below the resonances (0 eV, in Figure 8), the core-level signal is naturally zero and the comparison of the area-normalized spectra of Figure 6b in terms of intensity has to be made in relation to other features in the spectrum. From Figure 8 it is seen that 6 eV above the onset of the spectrum (corresponding to minimum in the high-energy end of region II in Figure 6b), contains completely different *p*-type PDOT for 1.5 and 18.8 M solutions. For 1.5 M a considerable density is seen whereas for 18.8 M the p-type transition density is much lower. This *decrease* of the p-type density of states as a function of concentration in the region II may explain the corresponding *relative increase* of the peak in region I, when H_2SO_4 concentration increases.

CONCLUSIONS

We have presented AIMD simulations of aqueous sulfuric acid over a wide concentration range from pure water to concentrated acid. The simulations were found to be in good agreement with our experimental results and values obtained from literature. We show results of NRIXS measurements of the O K edge and S $L_{2,3}$ edge core-excitation spectra for the same systems. The core-level excitations probe the local microscopic structure yielding a unique access to atomistic phenomena, like chemical bonding. The experimental results show changes in the O K edge spectra which support the structural findings of the AIMD simulations. Moreover, the S $L_{2,3}$ spectrum corresponds to the density-of-states calculations of the structures obtained from the AIMD simulations. The results reveal changes in hydrogen bonding of water molecules and the protonation state of the acid as a function of concentration. In particular, the number of donated hydrogen bonds per O_{water} increases from 1.9 of pure water to 2.5 of 18.0 M H_2SO_4(aq). Our results support the view that the systems consist of five components, H_2O, H_3O^+, H_2SO_4, HSO_4^-, and SO_4^{2-}, and we reveal their interplay as a function of concentration.

ASSOCIATED CONTENT

Supporting Information

This material is available free of charge via the Internet at http://pubs.acs.org/. The Supporting Information is available free of charge on the ACS Publications website at DOI: 10.1021/acs.jpcb.5b04371.

Radial distribution functions from the AIMD simulations, intensity curves of the spectral regions I–IV in Figure 4, a figure of the Gaussian fits performed to the S $L_{2,3}$ edge high-q spectra, and the simulated O K edge spectra (PDF)

AUTHOR INFORMATION

Corresponding Author

*(J.N.) E-mail: johannes.niskanen@helsinki.fi.

Present Address

§(S.L.) Chemical Sciences Division, Lawrence Berkeley National Laboratory, Berkeley, CA 94720.

Notes

The authors declare no competing financial interest.

ACKNOWLEDGMENTS

CSC-IT Center for Science Ltd., administered by the Ministry of Education, Science, and Culture is acknowledged for supercomputer resources for the project. Academy of Finland is acknowledged for funding through the projects 1260204 and 1259599. The authors thank the staff at European Synchrotron Radiation Facility, ESRF, Grenoble, France for their help in the project. The authors thank Prof. Hanna Vehkamäki and Dr. Ville Loukonen for invaluabe disscussions.

REFERENCES

(1) Berndt, T.; Böge, O.; Stratmann, F.; Heintzenberg, J.; Kulmala, M. Rapid Formation of Sulfuric Acid Particles at Near-Atmospheric Conditions. *Science* **2005**, *307*, 698–700.

(2) Almeida, J.; Schobesberger, S.; Kürten, A.; Ortega, I. K.; Kupiainen-Määttä, O.; Praplan, A. P.; Adamov, A.; Amorim, A.; Bianchi, F.; Breitenlechner, M.; et al. Molecular Understanding of Sulphuric Acid - Amine Particle Nucleation in the Atmosphere. *Nature* **2013**, *502*, 359–363.

(3) Intergovernmental Panel on Climate Change, Fifth Assessment Report: Climate Change 2013. http://www.ipcc.ch/report/ar5/, 2013 [Online; accessed 11 December, 2014].

(4) Bandy, A. R.; Ianni, J. C. Study of the Hydrates of H_2SO_4 Using Density Functional Theory. *J. Phys. Chem. A* **1998**, *102*, 6533–6539.

(5) Ianni, J. C.; Bandy, A. R. A Density Functional Theory Study of the Hydrates of $NH_3{\cdot}H_2SO_4$ and Its Implications for the Formation of New Atmospheric Particles. *J. Phys. Chem. A* **1999**, *103*, 2801–2811.

(6) Re, S.; Osamura, Y.; Morokuma, K. Coexistence of Neutral and Ion-Pair Clusters of Hydrated Sulfuric Acid $H_2SO_4(H_2O)_n$ (n = 1–5): A Molecular Orbital Study. *J. Phys. Chem. A* **1999**, *103*, 3535–3547.

(7) Larson, L. J.; Largent, A.; Tao, F.-M. Structure of the Sulfuric Acid-Ammonia System and the Effect of Water Molecules in the Gas Phase. *J. Phys. Chem. A* **1999**, *103*, 6786–6792.

(8) Ianni, J.; Bandy, A. A Theoretical Study of the Hydrates of $(H_2SO_4)_2$ and Its Implications for the Formation of New Atmospheric Particles. *J. Mol. Struct.: THEOCHEM* **2000**, *497*, 19–37.

(9) Miller, C. E.; Francisco, J. S. The Formation of a Surprisingly Stable HO_2 H_2SO_4 Complex. *J. Am. Chem. Soc.* **2001**, *123*, 10387–10388. PMID: 11603990

(10) Ding, C.-G.; Laasonen, K.; Laaksonen, A. Two Sulfuric Acids in Small Water Clusters. *J. Phys. Chem. A* **2003**, *107*, 8648–8658.

(11) Ding, C.-G.; Laasonen, K. Partially and Fully Deprotonated Sulfuric Acid in $H_2SO_4(H_2O)_n$(n = 6−9) clusters. *Chem. Phys. Lett.* **2004**, *390*, 307−313.
(12) Al Natsheh, A.; Nadykto, A. B.; Mikkelsen, K. V.; Yu, F.; Ruuskanen, J. Sulfuric Acid and Sulfuric Acid Hydrates in the Gas Phase:? A DFT Investigation. *J. Phys. Chem. A* **2004**, *108*, 8914−8929.
(13) Arrouvel, C.; Viossat, V.; Minot, C. Theoretical Study of Hydrated Sulfuric Acid: Clusters and Periodic Modeling. *J. Mol. Struct.: THEOCHEM* **2005**, *718*, 71−76.
(14) Miller, Y.; Chaban, G. M.; Gerber, R. B. Ab Initio Vibrational Calculations for H_2SO_4 and $H_2SO_4{\cdot}H_2O$: Spectroscopy and the Nature of the Anharmonic Couplings. *J. Phys. Chem. A* **2005**, *109*, 6565−6574.
(15) Nadykto, A. B.; Yu, F. Strong Hydrogen Bonding between Atmospheric Nucleation Precursors and Common Organics. *Chem. Phys. Lett.* **2007**, *435*, 14−18.
(16) Kurtén, T.; Torpo, L.; Ding, C.-G.; Vehkamäki, H.; Sundberg, M. R.; Laasonen, K.; Kulmala, M. A Density Functional Study on Water-Sulfuric Acid-Ammonia Clusters and Implications for Atmospheric Cluster Formation. *J. Geophys. Res.* **2007**, *112*, D04210.
(17) Anderson, K. E.; Siepmann, J. I.; McMurry, P. H.; VandeVondele, J. Importance of the Number of Acid Molecules and the Strength of the Base for Double-Ion Formation in $(H_2SO_4)_m{\cdot}$Base$\cdot(H_2O)_6$ Clusters. *J. Am. Chem. Soc.* **2008**, *130*, 14144−14147.
(18) Kurtén, T.; Loukonen, V.; Vehkamäki, H.; Kulmala, M. Amines Are Likely to Enhance Neutral and Ion-Induced Sulfuric Acid-Water Nucleation in the Atmosphere More Effectively than Ammonia. *Atmos. Chem. Phys.* **2008**, *8*, 4095−4103.
(19) Toivola, M.; Napari, I.; H, V. Structure of Water-Sulfuric Acid Clusters from Molecular Dynamics Simulations. *Boreal Env. Res.* **2009**, *14*, 654−661.
(20) Loukonen, V.; Kurtén, T.; Ortega, I. K.; Vehkamäki, H.; Pádua, A. A. H.; Sellegri, K.; Kulmala, M. Enhancing Effect of Dimethylamine in Sulfuric Acid Nucleation in the Presence of Water - A Computational Study. *Atmos. Chem. Phys.* **2010**, *10*, 4961−4974.
(21) Sugawara, S.; Yoshikawa, T.; Takayanagi, T.; Shiga, M.; Tachikawa, M. Quantum Proton Transfer in Hydrated Sulfuric Acid Clusters: A Perspective from Semiempirical Path Integral Simulations. *J. Phys. Chem. A* **2011**, *115*, 11486−11494.
(22) Partanen, L.; Hänninen, V.; Halonen, L. Ab Initio Structural and Vibrational Investigation of Sulfuric Acid Monohydrate. *J. Phys. Chem. A* **2012**, *116*, 2867−2879.
(23) Temelso, B.; Morrell, T. E.; Shields, R. M.; Allodi, M. A.; Wood, E. K.; Kirschner, K. N.; Castonguay, T. C.; Archer, K. A.; Shields, G. C. Quantum Mechanical Study of Sulfuric Acid Hydration: Atmospheric Implications. *J. Phys. Chem. A* **2012**, *116*, 2209−2224.
(24) Temelso, B.; Phan, T. N.; Shields, G. C. Computational Study of the Hydration of Sulfuric Acid Dimers: Implications for Acid Dissociation and Aerosol Formation. *J. Phys. Chem. A* **2012**, *116*, 9745−9758.
(25) Henschel, H.; Navarro, J. C. A.; Yli-Juuti, T.; Kupiainen-Määttä, O.; Olenius, T.; Ortega, I. K.; Clegg, S. L.; Kurtén, T.; Riipinen, I.; Vehkamäki, H. Hydration of Atmospherically Relevant Molecular Clusters: Computational Chemistry and Classical Thermodynamics. *J. Phys. Chem. A* **2014**, *118*, 2599−2611.
(26) Loukonen, V.; Kuo, I.-F.; McGrath, M.; Vehkamäki, H. On the Stability and Dynamics of (Sulfuric Acid);(Ammonia) and (Sulfuric Acid);(Dimethylamine) Clusters: A First-Principles Molecular Dynamics Investigation. *Chem. Phys.* **2014**, *428*, 164−174.
(27) Loukonen, V.; Bork, N.; Vehkamäki, H. From Collisions to Clusters: First Steps of Sulphuric Acid Nanocluster Formation Dynamics. *Mol. Phys.* **2014**, *112*, 1979−1986.
(28) Fiacco, D. L.; Hunt, S. W.; Leopold, K. R. Microwave Investigation of Sulfuric Acid Monohydrate. *J. Am. Chem. Soc.* **2002**, *124*, 4504−4511.
(29) Hintze, P. E.; Kjaergaard, H. G.; Vaida, V.; Burkholder, J. B. Vibrational and Electronic Spectroscopy of Sulfuric Acid Vapor. *J. Phys. Chem. A* **2003**, *107*, 1112−1118.
(30) Lund Myhre, C. E.; Christensen, D. H.; Nicolaisen, F. M.; Nielsen, C. J. Spectroscopic Study of Aqueous H_2SO_4 at Different Temperatures and Compositions:? Variations in Dissociation and Optical Properties. *J. Phys. Chem. A* **2003**, *107*, 1979−1991.
(31) Rozenberg, M.; Loewenschuss, A. Matrix Isolation Infrared Spectrum of the Sulfuric Acid Monohydrate Complex: New Assignments and Resolution of the Missing H-Bonded ν(OH) Band Issue. *J. Phys. Chem. A* **2009**, *113*, 4963−4971.
(32) Yacovitch, T. I.; Wende, T.; Jiang, L.; Heine, N.; Meijer, G.; Neumark, D. M.; Asmis, K. R. Infrared Spectroscopy of Hydrated Bisulfate Anion Clusters: $HSO_4^-(H_2O)_{1-16}$. *J. Phys. Chem. Lett.* **2011**, *2*, 2135−2140.
(33) Jubb, A. M.; Allen, H. C. Bisulfate Dehydration at Air/Solution Interfaces Probed by Vibrational Sum Frequency Generation Spectroscopy. *J. Phys. Chem. C* **2012**, *116*, 13161−13168.
(34) Yu, J.-J.; Zhang, Y.-H.; Li, Z.-S. Intermolecular Vibration Coupling between Libration of Water and ν_2-SOH for Clusters $HSO_4{-}(H_2O)_n$. *J. Phys. Chem. B* **2012**, *116*, 12597−12604.
(35) Margarella, A. M.; Perrine, K. A.; Lewis, T.; Faubel, M.; Winter, B.; Hemminger, J. C. Dissociation of Sulfuric Acid in Aqueous Solution: Determination of the Photoelectron Spectral Fingerprints of H_2SO_4, HSO_4, and SO_4^{2-} in Water. *J. Phys. Chem. C* **2013**, *117*, 8131−8137.
(36) Choe, Y.-K.; Tsuchida, E.; Ikeshoji, T. First-Principles Molecular Dynamics Study on Aqueous Sulfuric Acid Solutions. *J. Chem. Phys.* **2007**, *126*, 154510.
(37) Hammerich, A.; Buch, V.; Mohamed, F. Ab Initio Simulations of Sulfuric Acid Solutions. *Chem. Phys. Lett.* **2008**, *460*, 423−431.
(38) Choe, Y.-K.; Tsuchida, E.; Ikeshoji, T. Vibrational Analysis of Aqueous Sulfuric Acid: A Computational Study. *Int. J. Quantum Chem.* **2009**, *109*, 1984−1990.
(39) Vchirawongkwin, V.; Kritayakornupong, C.; Rode, B. M. Structural and Dynamical Properties and Vibrational Spectra of Bisulfate Ion in Water: A Study by Ab Initio Quantum Mechanical Charge Field Molecular Dynamics. *J. Phys. Chem. B* **2010**, *114*, 11561−11569.
(40) Ishiyama, T.; Morita, A. Molecular Dynamics Simulation of Sum Frequency Generation Spectra of Aqueous Sulfuric Acid Solution. *J. Phys. Chem. C* **2011**, *115*, 13704−13716.
(41) Hammerich, A. D.; Buch, V. Ab Initio Molecular Dynamics Simulations of the Liquid/Vapor Interface of Sulfuric Acid Solutions. *J. Phys. Chem. A* **2012**, *116*, 5637−5652.
(42) Fraenkel, D. Electrolytic Nature of Aqueous Sulfuric Acid. 1. Activity. *J. Phys. Chem. B* **2012**, *116*, 11662−11677.
(43) Fraenkel, D. Electrolytic Nature of Aqueous Sulfuric Acid. 2. Acidity. *J. Phys. Chem. B* **2012**, *116*, 11678−11686.
(44) Schülke, W. *Electron Dynamics by Inelastic X-Ray Scattering, Oxford Series on Synchrotron Radiation*; Oxford University Press: Oxford, U.K., 2004.
(45) Inkinen, J.; Niskanen, J.; Sakko, A.; Ruotsalainen, K. O.; Pylkkänen, T.; Galambosi, S.; Hakala, M.; Monaco, G.; Hämäläinen, K.; Huotari, S. Interplay between Temperature-Activated Vibrations and Nondipolar Effects in the Valence Excitations of the CO_2 Molecule. *J. Phys. Chem. A* **2014**, *118*, 3288−3294.
(46) Sahle, C. J.; Sternemann, C.; Schmidt, C.; Lehtola, S.; Jahn, S.; Simonelli, L.; Huotari, S.; Hakala, M.; Pylkkänen, T.; Nyrow, A.; et al. Microscopic structure of water at elevated pressures and temperatures. *Proc. Natl. Acad. Sci. U. S. A.* **2013**, *110*, 6301−6306.
(47) Beamline ID20 at the European Synchrotron Radiation Facility, Grenoble, France, web page. http://www.esrf.eu/home/UsersAndScience/Experiments/Beamlines/content/content/ID20.html, [Online; accessed 11-December- 2014].
(48) Marx, D.; Hutter, J. *Ab Initio Molecular Dynamics - Basic Theory and Advanced Methods*; Cambridge University Press: Cambridge, U.K., 2009.
(49) The CP2K Developers Group. http://www.cp2k.org/ [Online; accessed 11 December, 2014].
(50) Hutter, J.; Iannuzzi, M.; Schiffmann, F.; VandeVondele, J. CP2K: Atomistic Simulations of Condensed Matter Systems. *Wiley*

DOI: 10.1021/acs.jpcb.5b04371
J. Phys. Chem. B XXXX, XXX, XXX−XXX

Interdisciplinary Reviews: Computational Molecular Science **2014**, *4*, 15−25.
(51) Perdew, J.; Burke, K.; Ernzerhof, M. Generalized Gradient Approximation Made Simple. *Phys. Rev. Lett.* **1996**, *77*, 3865−3868.
(52) VandeVondele, J.; Krack, M.; Mohamed, F.; Parrinello, M.; Chassaing, T.; Hutter, J. Quickstep: Fast and Accurate Density Functional Calculations Using a Mixed Gaussian and Plane Waves Approach. *Comput. Phys. Commun.* **2005**, *167*, 103−128.
(53) Goedecker, S.; Teter, M.; Hutter, J. Separable Dual-Space Gaussian Pseudopotentials. *Phys. Rev. B: Condens. Matter Mater. Phys.* **1996**, *54*, 1703−1710.
(54) Knopf, D. A.; Luo, B. P.; Krieger, U. K.; Koop, T. Thermodynamic Dissociation Constant of the Bisulfate Ion from Raman and Ion Interaction Modeling Studies of Aqueous Sulfuric Acid at Low Temperatures. *J. Phys. Chem. A* **2003**, *107*, 4322−4332.
(55) Walrafen, G.; Yang, W.-H.; Chu, Y.; Hokmabadi, M. Structures of Concentrated Sulfuric Acid Determined from Density, Conductivity, Viscosity, and Raman Spectroscopic Data. *J. Solution Chem.* **2000**, *29*, 905−936.
(56) Wernet, P.; Nordlund, D.; Bergmann, U.; Cavalleri, M.; Odelius, M.; Ogasawara, H.; Näslund, L. Å; Hirsch, T. K.; Ojamäe, L.; Glatzel, P.; et al. The Structure of the First Coordination Shell in Liquid Water. *Science* **2004**, *304*, 995−999.
(57) Pylkkänen, T.; Sakko, A.; Hakala, M.; Hämäläinen, K.; Monaco, G.; Huotari, S. Temperature Dependence of the Near-Edge Spectrum of Water. *J. Phys. Chem. B* **2011**, *115*, 14544−14550.
(58) Cai, Y. Q.; Mao, H.-K.; Chow, P. C.; Tse, J. S.; Ma, Y.; Patchkovskii, S.; Shu, J. F.; Struzhkin, V.; Hemley, R. J.; Ishii, H.; et al. Ordering of Hydrogen Bonds in High-Pressure Low-Temperature H_2O. *Phys. Rev. Lett.* **2005**, *94*, 025502.
(59) Huang, C.; Wikfeldt, K. T.; Tokushima, T.; Nordlund, D.; Harada, Y.; Bergmann, U.; Niebuhr, M.; Weiss, T. M.; Horikawa, Y.; Leetmaa, M.; et al. The Inhomogeneous Structure of Water at Ambient Conditions. *Proc. Natl. Acad. Sci. U. S. A.* **2009**, *106*, 15214−15218.
(60) Nilsson, A.; Nordlund, D.; Waluyo, I.; Huang, N.; Ogasawara, H.; Kaya, S.; Bergmann, U.; Näslund, L.-Å; Öström, H.; Wernet, P.; et al. X-ray Absorption Spectroscopy and X-ray Raman Scattering of Water and Ice; an Experimental View. *J. Electron Spectrosc. Relat. Phenom.* **2010**, *177*, 99−129.
(61) Pylkkänen, T.; Giordano, V. M.; Chervin, J.-C.; Sakko, A.; Hakala, M.; Soininen, J. A.; Hämäläinen, K.; Monaco, G.; Huotari, S. Role of Non-Hydrogen-Bonded Molecules in the Oxygen K-Edge Spectrum of Ice. *J. Phys. Chem. B* **2010**, *114*, 3804−3808.
(62) Juurinen, I.; Pylkkänen, T.; Ruotsalainen, K. O.; Sahle, C. J.; Monaco, G.; Hämäläinen, K.; Huotari, S.; Hakala, M. Saturation Behavior in X-ray Raman Scattering Spectra of Aqueous LiCl. *J. Phys. Chem. B* **2013**, *117*, 16506−16511.
(63) Velasco-Velez, J.-J.; Wu, C. H.; Pascal, T. A.; Wan, L. F.; Guo, J.; Prendergast, P.; Salmeron, M. The Structure of Interfacial Water on Gold Electrodes Studied by X-ray Absorption Spectroscopy. *Science* **2014**, *346*, 831−834.
(64) Tse, J. S.; Shaw, D. M.; Klug, D. D.; Patchkovskii, S.; Vankó, G.; Monaco, G.; Krisch, M. X-ray Raman Spectroscopic Study of Water in the Condensed Phases. *Phys. Rev. Lett.* **2008**, *100*, 095502.
(65) Chen, W.; Wu, X.; Car, R. X-ray Absorption Signatures of the Molecular Environment in Water and Ice. *Phys. Rev. Lett.* **2010**, *105*, 017802.
(66) Kaya, S.; Schlesinger, D.; Yamamoto, S.; Newberg, J. T.; Bluhm, H.; Ogasawara, H.; Kendelewicz, T.; Brown, G. E.; Pettersson, L. G. M.; Nilsson, A. Highly Compressed Two-Dimensional Form of Water at Ambient Conditions. *Sci. Rep.* **2013**, *3* (1074), 1−5.
(67) Triguero, L.; Pettersson, L. G. M.; Ågren, H. Calculations of Near-Edge X-Ray-Absorption Spectra of Gas-Phase and Chemisorbed Molecules by Means of Density-Functional and Transition-Potential Theory. *Phys. Rev. B: Condens. Matter Mater. Phys.* **1998**, *58*, 8097−8110.
(68) Iannuzzi, M.; Hutter, J. Inner-Shell Spectroscopy by the Gaussian and Augmented Plane Wave Method. *Phys. Chem. Chem. Phys.* **2007**, *9*, 1599−1610.

DOI: 10.1021/acs.jpcb.5b04371
J. Phys. Chem. B XXXX, XXX, XXX−XXX